

Visualization of Myocardial Phosphoinositide Turnover with 1-[1-¹¹C]-Butyryl-2-Palmitoyl-rac-Glycerol in Rats with Myocardial Infarction

Masanobu Chida, Yutaka Kagaya, Yoshio Imahori, Shigeto Namiuchi, Ryou Fujii, Mitsumasa Fukuchi, Chikako Takahashi, Fumiaki Tezuka, Tatsuo Ido, and Kunio Shirato

Department of Cardiovascular Medicine, Tohoku University Graduate School of Medicine, Sendai; Department of Neurosurgery, Kyoto Prefectural University of Medicine, Kyoto; Cyclotron Unit, Nishijin Hospital, Kyoto; Department of Pathology, National Sendai Hospital, Sendai; and Cyclotron and Radioisotope Center, Tohoku University, Sendai, Japan

Phosphoinositide turnover mediates the signaling of angiotensin II, which plays a pivotal role in ventricular remodeling after myocardial infarction (MI). We tested the hypothesis that phosphoinositide turnover can be visualized by 1-[1-¹¹C]butyryl-2-palmitoyl-rac-glycerol (¹¹C-DAG) in both infarcted and noninfarcted myocardium after MI in rats. **Methods:** Rats received an injection of ¹¹C-DAG 7 d after left coronary artery ligation, and myocardial lipids were extracted from both infarcted and noninfarcted areas of myocardium (n = 3). Metabolites of ¹¹C-DAG were determined by thin-layer chromatography. Quantitative autoradiography of hearts was performed to visualize myocardial phosphoinositide turnover in rats that received an injection of ¹¹C-DAG 1 d (n = 3) and 7 d (n = 5) after MI and 7 d after a sham operation (n = 3). Quantitative autoradiography with ²⁰¹TlCl was also performed to evaluate myocardial blood flow in rats 7 d after MI (n = 3). Cells occupying the infarcted myocardium were identified by immunohistochemistry. **Results:** The radioactivity incorporated into the intermediates of phosphoinositide turnover was predominant in both the infarcted (67.1% ± 5.2% of the total activity) and the noninfarcted (57.4% ± 3.2%) myocardium. ¹¹C-DAG radioactivity in the infarcted region normalized to that in the noninfarcted region was 1.09 ± 0.04 in rats 7 d after MI, which was significantly higher than that in rats 1 d after MI (0.38 ± 0.03, *P* < 0.001). ²⁰¹Tl radioactivity in the infarcted region normalized to that in the noninfarcted region was only 0.19 ± 0.01 7 d after MI. ¹¹C-DAG radioactivity in the noninfarcted region normalized to that in the right ventricular free wall tended to be increased in rats 1 and 7 d after MI compared with the sham-operated rats; the differences, however, were not statistically significant (1.30 ± 0.15, 1.20 ± 0.07, and 1.13 ± 0.02, respectively). Immunohistochemistry revealed that abundant fibroblasts, myofibroblasts, and macrophages occupied the infarcted myocardium 7 d after MI, but the cellularity was low during the first day after MI. **Conclusion:** These data suggest that ¹¹C-DAG may be useful for visualizing regions with activated phosphoinositide turnover after MI. Because wound healing and fibrogenic processes are important factors of ventricular remodeling, ¹¹C-DAG and PET may offer new information benefiting patient management after MI.

Key Words: myocardial infarction; ventricular remodeling; phosphoinositide turnover

J Nucl Med 2000; 41:2063–2068

Left ventricular remodeling, expansion of the infarct zone, and changes in the noninfarcted myocardium greatly affect ventricular function and prognosis in patients who survive after myocardial infarction (MI) (1). Angiotensin-converting enzyme inhibitors have been shown to improve the depressed left ventricular function or prognosis after MI (2–4). These findings suggest that angiotensin II, the receptors for which are expressed predominantly in the infarcted area with active fibrogenesis rather than in the noninfarcted area (5–7), plays a pivotal role in the process of left ventricular remodeling after MI.

Phosphoinositide turnover and its two second messengers, inositol 1,4,5-trisphosphate and 1,2-diacylglycerol (8), have been shown to mediate angiotensin II signaling in many kinds of cells, including both cardiac myocytes and fibroblasts (9,10). An estimation of the myocardial phosphoinositide turnover activity, which may be closely linked to the process of ventricular remodeling after MI, should therefore be helpful. In previous studies (11–14), we showed regional alterations of phosphoinositide turnover in the neurotransmission process using PET and 1-[1-¹¹C]butyryl-2-palmitoyl-rac-glycerol (¹¹C-DAG), a ¹¹C-labeled diacylglycerol. In this study, we investigated whether the phosphoinositide turnover activity in both infarcted and noninfarcted regions can be visualized with ¹¹C-DAG in rats after MI.

MATERIALS AND METHODS

Animals and Radiopharmaceutical

The experiments were performed according to the guidelines for the care and use of laboratory animals of our institutions. The left coronary artery of 8-wk-old male Wistar rats (Funabashi Farms, Shizuoka, Japan) was ligated. The rats were anesthetized with sodium pentobarbital (50 mg/kg intraperitoneally), intubated, and ventilated through an endotracheal tube attached to a respirator.

Received Jan. 10, 2000; revision accepted May 16, 2000.

For correspondence or reprints contact: Kunio Shirato, MD, PhD, Department of Cardiovascular Medicine, Tohoku University Graduate School of Medicine, 1-1 Seiryomachi, Aoba-ku, Sendai, 980-8574 Japan.

Through a left-sided thoracotomy, the left coronary artery was ligated with a 6-0 silk suture. In sham-operated rats, the chest and the pericardium were opened, but the coronary artery was not ligated. ^{11}C -DAG (specific activity, 186 GBq/ μmol) was synthesized by the ketene method as previously reported (11) and was dissolved in saline with 25% human serum albumin for intravenous injection. $^{201}\text{TlCl}$ for autoradiography was purchased from Nihon Mediphysics (Osaka, Japan).

^{11}C -DAG Metabolites

To confirm the validity of ^{11}C -DAG as a probe specific to myocardial phosphoinositide turnover, we injected 0.74–2.22 GBq ^{11}C -DAG into the rats through the tail vein 7 d after MI ($n = 3$). Thirty minutes after the injection, the rats were killed by ether inhalation and the hearts were removed. Both infarcted and noninfarcted myocardium was dissected from visually identified scar tissue and nonscar tissue, respectively. Myocardial lipids were extracted by a previously reported (13) modification of Folch's method. Briefly, samples of the infarcted and noninfarcted myocardium were homogenized separately by grinding with 0.5 mL solvent (chloroform:methanol, 3:2, volume in volume) and centrifuged at 3000 rpm at 10°C for 3 min. The supernatant containing lipids was spotted on thin-layer chromatography plates (Silica Gel 60; Whatman International, Maidstone, UK) that had been activated for 1 h at 100°C before use. The solvent system was chloroform:methanol:ammonium hydroxide:water, 20:15:3:2, volume in volume.

The developed thin-layer chromatography plates were put into contact with general-use imaging plates (Fuji Photo Film, Tokyo, Japan) and exposed for 1 h (15). The positions of the various phospholipid radioactivities were visualized and quantified using an image-processing system (BAS2000; Fuji Photo Film). The thin-layer chromatography plates were also exposed to iodine vapors to reveal the authentic compounds, which consisted of 1,2-diacylglycerol, phosphatidylcholine, phosphatidylethanolamine, phosphatidic acid, phosphatidylinositol, phosphatidylinositol-4-monophosphate, phosphatidylinositol-4,5-bisphosphate, and butyryl coenzyme A (CoA). We calculated the percentage of the fraction of each ^{11}C -labeled metabolite as follows: autoradiographic intensity of each fraction/sum of intensities of all fractions $\times 100$ (%).

Quantitative Autoradiography

In vivo quantitative autoradiography was performed as described previously (15,16). We injected 185 MBq ^{11}C -DAG into the rats through the tail vein 1 ($n = 3$) and 7 ($n = 5$) d after MI and 7 d after the sham operation ($n = 3$). Thirty minutes after the injection, the rats were killed by ether inhalation. The hearts were then removed and frozen with powdered dry ice. Forty-micrometer sections taken perpendicular to the long axis of the left ventricle at the midventricular level were prepared using a cryomicrotome at -20°C . The sections were mounted on cover slides, dried on a hot plate, and exposed to imaging plates for 1 h. These sections were also stained with hematoxylin–eosin after the exposure to identify both infarcted and noninfarcted regions of myocardium. A section containing the largest infarcted region was selected from each heart, and the autoradiographic intensity was measured by the BAS2000 system. Consecutive circular regions of interest were placed circumferentially on both infarcted (0.2 mm² in area) and noninfarcted (1.0 mm² in area) regions as well as on the right ventricular free wall (0.2 mm² in area). For the sham-operated rats, circular regions of interest were placed on the interventricular

septum (1.0 mm² in area) and the right ventricular free wall (0.2 mm² in area). To estimate the myocardial blood flow distribution in rats 7 d after MI, we performed quantitative autoradiography with $^{201}\text{TlCl}$. Ten minutes after the injection of 17.5 MBq $^{201}\text{TlCl}$ ($n = 3$), the hearts were removed and processed as described in the previous section. The sections (20 μm) were exposed to imaging plates for 1.5 h. The autoradiographic intensity was measured by the BAS3000 system.

Immunohistochemistry

Immunohistochemical analysis was performed on 4 hearts 7 d after MI. For the staining of vimentin and α -smooth muscle actin, the hearts were fixed with neutral buffered 10% formalin after isolation and embedded in paraffin. Sections (2.5 μm) were incubated overnight with murine monoclonal antivimentin or anti- α -smooth muscle actin antibodies (DAKO, Glostrup, Denmark) at a dilution of 1:100 in phosphate-buffered saline solution containing 1% bovine serum albumin. After being washed in phosphate-buffered saline solution for 15 min, the sections were incubated with biotinylated horse antimouse IgG (Vector Laboratories Inc., Burlingame, CA) for 30 min and finally with streptavidin–peroxidase complex (DAKO) for 30 min. The color was developed with diaminobenzidine.

For the staining of ED-1, smooth muscle myosin heavy chain, and von Willebrand factor, the hearts were frozen with liquid nitrogen after isolation. Cryostat sections (4 μm) were fixed with periodate–lysine–paraformaldehyde for 30 min. They were then incubated with murine monoclonal antirat mononuclear phagocyte (anti-ED-1) antibody (Pharmingen, San Diego, CA) at a dilution of 1:800, murine monoclonal antirat smooth muscle myosin heavy chain (Santa Cruz Biotechnology, Santa Cruz, CA) at a dilution of 1:200, or rabbit antihuman von Willebrand factor (DAKO) at a dilution of 1:1500. The sections were processed further for immunostaining as described previously (17).

Statistical Analysis

Statistical analysis was performed using ANOVA for comparison among 3 groups or an unpaired Student *t* test for comparison between 2 groups. Values are presented as mean \pm SEM. $P < 0.05$ was considered significant.

RESULTS

^{11}C -DAG Metabolites

Figure 1 shows a representative thin-layer chromatography profile of ^{11}C -DAG metabolites obtained from the infarcted and noninfarcted myocardium in a rat 7 days after MI. Figure 2 summarizes the incorporation of ^{11}C radioactivity into various metabolites of ^{11}C -DAG. Phosphatidic acid, phosphatidylinositol, phosphatidylinositol-4-monophosphate, and phosphatidylinositol-4,5-bisphosphate, which are the intermediates of phosphoinositide turnover, were the predominant metabolites. The percentage of the sum of the intermediates of phosphoinositide turnover was $67.1\% \pm 5.2\%$ in the infarcted myocardium and $57.4\% \pm 3.2\%$ in the noninfarcted myocardium. In both the infarcted and noninfarcted myocardium, phosphatidylcholine and phosphatidylethanolamine appeared as less than 5% of the total radioactivity. The percentage of the butyryl CoA fraction, which is a product of the degradation of ^{11}C -DAG by lipase,

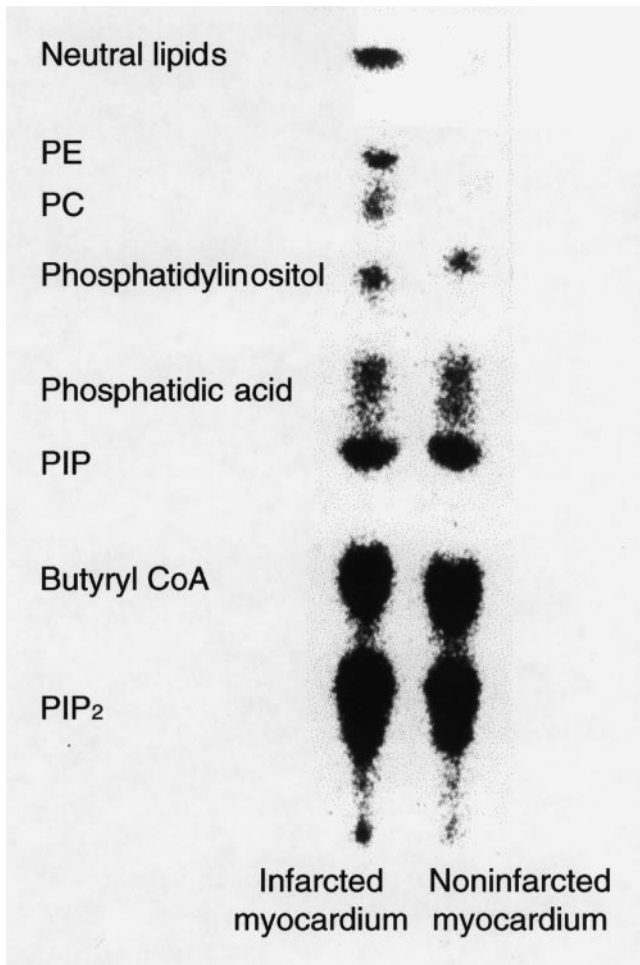


FIGURE 1. Thin-layer chromatography profiles of ¹¹C-DAG metabolites obtained from infarcted and noninfarcted myocardium 7 d after MI. PC = phosphatidylcholine; PE = phosphatidylethanolamine; PIP = phosphatidylinositol-4-monophosphate; PIP₂ = phosphatidylinositol-4,5-bisphosphate.

was $22.9\% \pm 1.2\%$ in the infarcted myocardium, and $34.9\% \pm 8.1\%$ in the noninfarcted myocardium.

Quantitative Autoradiography

Figure 3A shows a representative autoradiograph of a heart obtained from a rat in which ¹¹C-DAG was injected 7 d after the sham operation. The ¹¹C-DAG distribution in the left ventricle was homogeneous. Figure 3B shows a representative autoradiograph obtained from a rat in which ¹¹C-DAG was injected 1 d after MI. The autoradiographic intensity was low in the infarcted region. As shown in Figure 3C, the autoradiographic intensity was extremely low in the infarcted region in rats that received a ²⁰¹TlCl injection 7 d after MI. In contrast, as shown in Figure 3D, the autoradiographic intensity of ¹¹C-DAG in the infarcted region was comparable with or even slightly higher than that in the noninfarcted region in rats 7 d after MI. ¹¹C-DAG radioactivity in the infarcted region normalized to that in the noninfarcted region was 1.09 ± 0.04 in rats 7 d after MI. This value was significantly higher than that in rats 1 d after MI

(0.38 ± 0.03 , $P < 0.001$) (Fig. 4). The result was the same when we normalized the radioactivity in the infarcted region to that in the right ventricular free wall (1.31 ± 0.09 versus 0.49 ± 0.03 , $P < 0.001$). The radioactivity in the infarcted region normalized to that in the noninfarcted myocardium was also higher for ¹¹C-DAG than for ²⁰¹Tl in rats 7 days after MI (1.09 ± 0.04 versus 0.19 ± 0.01 , $P < 0.001$; Fig. 4). ¹¹C-DAG radioactivity in the noninfarcted myocardium normalized to that in the right ventricular free wall tended to be increased in rats 1 and 7 d after MI compared with sham-operated rats; the differences, however, were not statistically significant (1.30 ± 0.15 , 1.20 ± 0.07 , and 1.13 ± 0.02 , respectively; Fig. 5).

Immunohistochemistry 7 Days After MI

Histologic examination using sections stained with hematoxylin–eosin revealed abundant cells similar to fibroblasts and macrophages surrounding the necrotic myocytes in the infarcted region 7 d after MI (Fig. 6A). Immunohistochemical analysis showed that almost all cells surrounding the necrotic myocytes were positively stained for vimentin and that some of these cells were also labeled for α -smooth muscle actin or for ED-1 but not for smooth muscle myosin heavy chain or von Willebrand factor (Fig. 6). The relatively high background level in the staining for smooth muscle myosin heavy chain was the same as for the negative control (data not shown). These data suggest that the predominant cells in the infarcted region 7 d after MI were myofibroblasts (α -smooth muscle actin–positive), macrophages (ED-1–positive), and fibroblasts (vimentin–positive and both α -smooth muscle actin–negative and ED-1–negative).

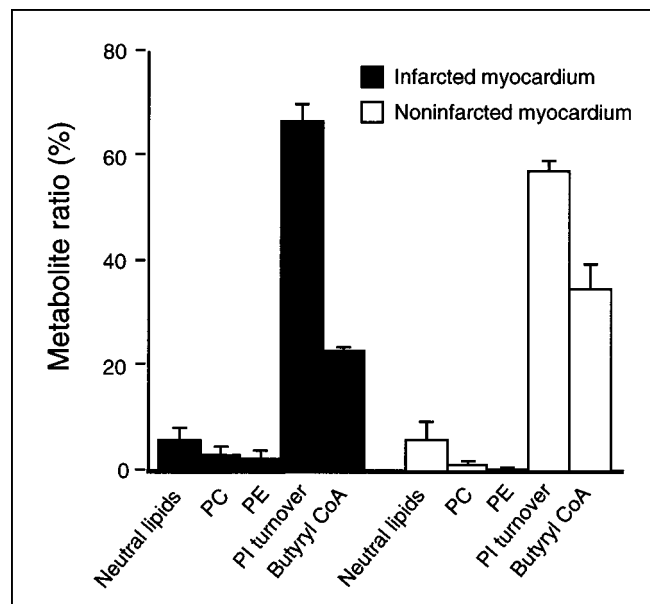


FIGURE 2. Incorporation of ¹¹C radioactivity into various metabolites of ¹¹C-DAG in infarcted and noninfarcted myocardium 7 d after coronary ligation. PC = phosphatidylcholine; PE = phosphatidylethanolamine; PI = phosphatidylinositol. Bars represent mean \pm SEM.

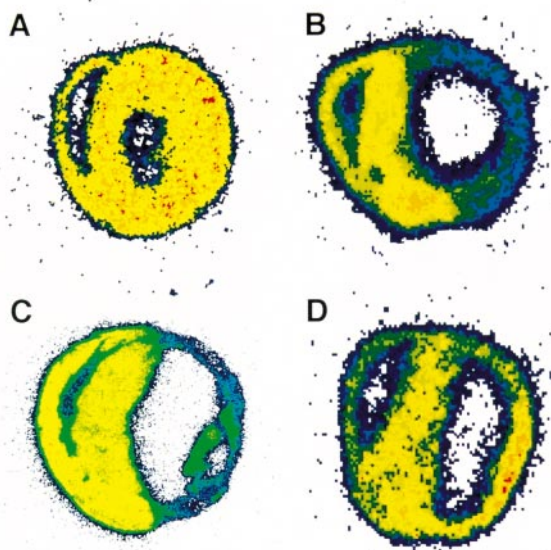


FIGURE 3. Representative autoradiographs of ^{11}C -DAG distribution in rat heart 7 d after sham operation (A), ^{11}C -DAG distribution in rat heart 1 d after coronary ligation (B), ^{201}Tl distributions in rat heart 7 d after coronary ligation (C), and ^{11}C -DAG distributions in rat hearts 7 d after coronary ligation (D). In each image, right ventricular free wall is at upper left, interventricular septum is at middle, and left ventricular free wall is at lower right.

DISCUSSION

The incorporation of ^{11}C radioactivity into the intermediates of phosphoinositide turnover was the predominant metabolic fate of ^{11}C -DAG both in the infarcted and in the noninfarcted myocardium in rats 7 d after MI. The *in vivo* quantitative autoradiography with ^{11}C -DAG revealed that the radioactivity in the infarcted region was low 1 d after MI and increased remarkably 7 d after, even though the blood flow distribution in this area was limited. These findings suggest that phosphoinositide turnover is activated in the healing and fibrogenic process after MI. These results agree with those of a recent study by Ju et al. (18) showing that the $G_{q\alpha}$ /phospholipase C- β_1 pathway, the upstream signaling system for phosphoinositide turnover, is upregulated predominantly in scar tissue in rats 8 wk after MI. In our study, histologic examination revealed that abundant fibroblasts, myofibroblasts, and macrophages occupied the infarcted myocardium 7 d after MI. On the other hand, the cellularity was extremely low 1 d after MI. Earlier studies by others underscored the role of phosphoinositide turnover in the activation of fibroblasts (10), myofibroblasts (19), and macrophages (20), suggesting that these cells are responsible for the accelerated ^{11}C -DAG distribution in the infarcted region. We observed a few live cardiac myocytes in the subendocardial layer of the infarcted region. These cardiac myocytes may partially explain the increased ^{11}C -DAG radioactivity in the infarcted region.

The reason for the minimal differences in ^{11}C -DAG distribution among the noninfarcted regions 1 and 7 d after MI and the myocardium 7 d after the sham operation is not clear. In our preliminary study, heart weight significantly increased by 13% in rats 7 d after MI compared with sham-operated rats. The hypertrophic response in noninfarcted myocardium, therefore, should be initiated at this time after MI. This observation has several possible explanations. First, as suggested by Ju et al. (18), the contribution of phosphoinositide turnover to the process of left ventricular remodeling may be less important in noninfarcted myocardium than in infarcted myocardium. This notion may be further supported by our recent report (21) in which ^3H -labeled phorbol 12,13-dibutyrate binding was significantly greater in infarcted tissue than in noninfarcted myocardium but was similar in noninfarcted myocardium and in myocardium from sham-operated rats. These data suggest that protein kinase C, which is in the downstream pathway of phosphoinositide turnover, may be activated in the infarcted tissue but not in the noninfarcted tissue. Second, in our preliminary experiment, the average infarct size of our experimental MI model was 38% of the total left ventricle, and no rats in this study had apparent signs of heart failure. We may need more extensive MI to detect a significant increase in the ^{11}C -DAG distribution in noninfarcted myocardium. Third, the percentage of the butyryl CoA fraction, which is a product of the degradation of ^{11}C -DAG by lipase, tended to be higher in the noninfarcted myocardium than in the infarcted myocardium. Therefore, the phosphoinositide turnover activity in the noninfarcted myocardium may have been underestimated.

Our data may not agree with earlier reports showing that

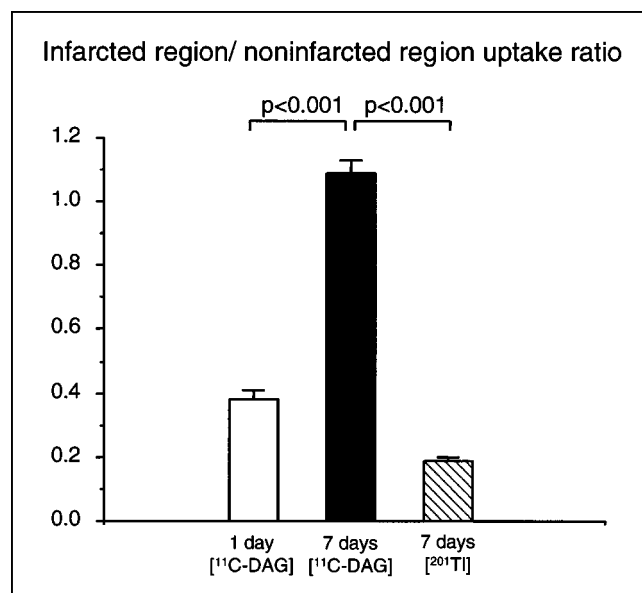


FIGURE 4. Ratio of radioactivity in infarcted region normalized to that in noninfarcted region in rats injected with ^{11}C -DAG 1 and 7 d after coronary ligation and in rats injected with ^{201}Tl 7 d after coronary ligation. Values are mean \pm SEM.

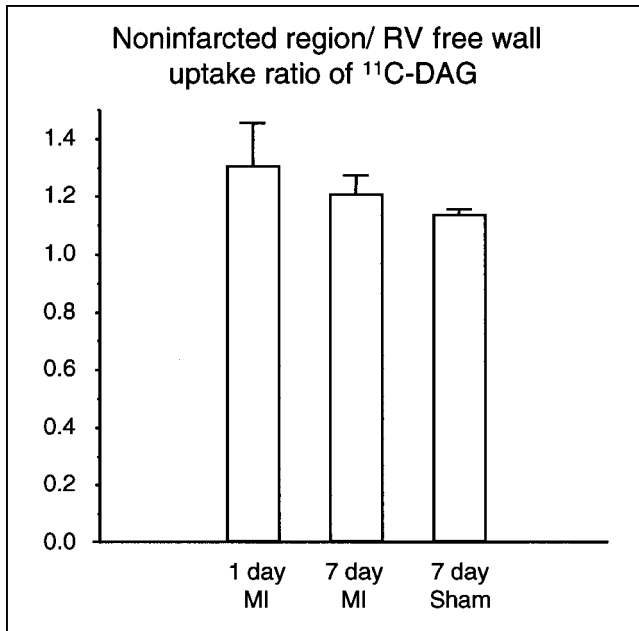


FIGURE 5. Ratio of ¹¹C-DAG uptake in noninfarcted region to that in right ventricular (RV) free wall in rats 1 and 7 d after coronary ligation (MI) and 7 d after sham operation (Sham). Values are mean ± SEM.

phosphoinositide turnover plays a pivotal role in the hypertrophic response in cultured neonatal rat cardiac myocytes stimulated by mechanical stretch (22), endothelin-1 (23), α_1 -adrenergic stimulation (24), and angiotensin II (9). The difference between our results and those of others may be caused by differences between adult and neonatal cardiac myocytes or differences between long-term in vivo and short-term in vitro experimental models. In contrast, our findings for the noninfarcted myocardium are consistent with a recent report by Ju et al. (18) showing that upregulation of the upstream signaling pathway for phosphoinositide turnover is apparently less prominent in noninfarcted myo-

cardium than in infarcted myocardium. Our results, however, partially conflict with those of Ju et al. because Ju et al. showed that $G_{q\alpha}$ mRNA and the phospholipase C- β_1 protein level were slightly but significantly increased in noninfarcted myocardium compared with those in sham-operated rats, although the increase was apparently less prominent than that in the scar tissue and the $G_{q\alpha}$ protein level was not increased. Differences in the methods used for the estimation of phosphoinositide turnover may explain the slight differences in our results from those of Ju et al.

This study has several possible limitations. First, the ¹¹C-DAG supplied to the infarcted myocardium is probably low because the blood flow in the infarcted area is low. ¹¹C-DAG radioactivity in the infarcted region, therefore, should be interpreted carefully. We may have underestimated the phosphoinositide turnover activity in the infarcted region because of the limited blood supply. Second, because we did not measure absolute counts in the myocardium and plasma, we could not obtain the ¹¹C-DAG uptake expressed as a percentage of the injected dose, the uptake normalized by flow, or data analyzed by a kinetic model. Third, in the ¹¹C-DAG metabolite study, ¹¹C-butyryl CoA, which is a product of the degradation of ¹¹C-DAG by lipase and is not an intermediate of phosphoinositide turnover, was the second predominant metabolite of ¹¹C-DAG. In our previous study, we showed that ¹¹C-butyryl CoA appeared in the plasma 10 min after the injection (11), suggesting that a part of butyryl CoA in the myocardium was derived from plasma ¹¹C-butyryl CoA. It is also possible that ¹¹C-butyryl CoA was produced by lipase in cardiac myocytes and cells in the infarcted myocardium after ¹¹C-DAG was taken into those cells (25). Finally, because the infarcted myocardium in rats 7 d after MI was occupied by macrophages, myofibroblasts, and fibroblasts, all 3 of these types of cells may have contributed to ¹¹C-DAG uptake in this area. Although macrophages play a pivotal role in scavenging necrotic myocytes, and phosphoinositide turnover is suggested to

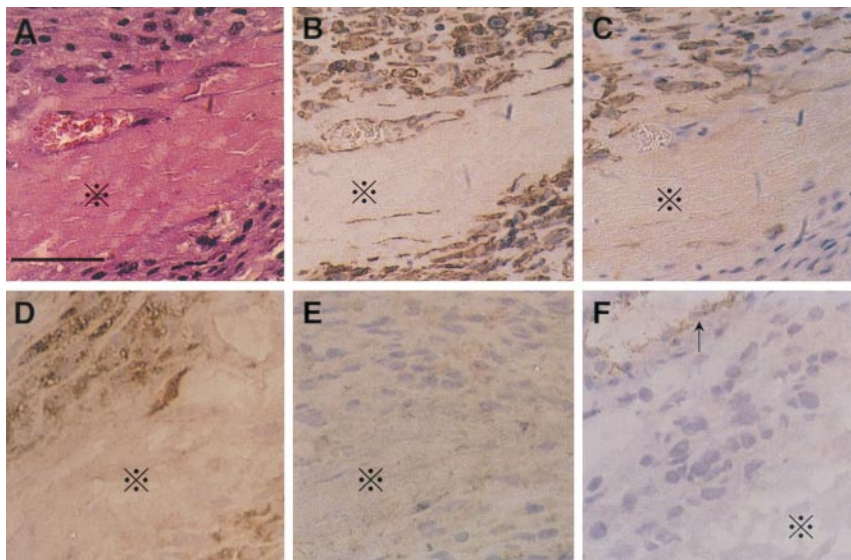


FIGURE 6. Hematoxylin-eosin staining (A) and immunohistochemical labeling for vimentin (B), α -smooth muscle actin (C), ED-1 (D), smooth muscle myosin heavy chain (E), and von Willebrand factor (F) in infarcted area in rat 7 d after MI. Necrotic myocytes (*) are surrounded by spindle-shaped cells similar to fibroblasts and macrophages. Almost all these cells were stained for vimentin. Some were also labeled for α -smooth muscle actin or for ED-1 but not for smooth muscle myosin heavy chain or von Willebrand factor (except for vascular endothelial cells [arrow]). Relatively high background level in staining for smooth muscle myosin heavy chain was same as in negative control. Scale bar represents 50 μ m.

play an important role in the activation of macrophages (20), we cannot determine the relative contribution of phosphoinositide turnover by macrophages to the total phosphoinositide turnover activity.

A further study to analyze the uptake of ^{11}C -DAG by cells in more detail, such as by a kinetic model, as well as a study to identify which cells are responsible for the increased ^{11}C -DAG uptake, is required. An investigation to determine the effect of angiotensin-converting enzyme inhibitor or angiotensin II type 1 receptor blockade is also needed. Because the final goal is to visualize myocardial phosphoinositide turnover in humans using PET, a study that measures ^{11}C -DAG uptake by the liver to assess the impact of liver metabolism on imaging in vivo is also required.

CONCLUSION

The results of this study suggest that ^{11}C -DAG may be useful for visualizing regions with activated phosphoinositide turnover after MI. Because wound healing and the fibrogenic process are important factors of ventricular remodeling after MI, ^{11}C -DAG and PET may offer new information that benefits patient management after MI.

ACKNOWLEDGMENTS

The authors thank Brent Bell for reading the manuscript. This study was supported in part by grants-in-aid for science research 07670747, 11670657, 08671602, 09671439, and 07557065 from the Ministry of Education, Science, Sports, and Culture of Japan.

REFERENCES

1. Pfeffer MA, Braunwald E. Ventricular remodeling after myocardial infarction: experimental observations and clinical implications. *Circulation*. 1990;81:1161–1172.
2. Pfeffer MA, Pfeffer JM, Steinberg C, Finn P. Survival after experimental myocardial infarction: beneficial effects of long-term therapy with captopril. *Circulation*. 1985;72:406–412.
3. Pfeffer MA, Braunwald E, Moye LA, et al. Effect of captopril on mortality and morbidity in patients with left ventricular dysfunction after myocardial infarction: results of the survival and ventricular enlargement trial. *N Engl J Med*. 1992;327:669–677.
4. The Acute Infarction Ramipril Efficacy (AIRE) Study Investigators. Effect of ramipril on mortality and morbidity of survivors of acute myocardial infarction with clinical evidence of heart failure. *Lancet*. 1993;342:821–828.
5. Sun Y, Weber KT. Angiotensin II receptor binding following myocardial infarction in the rat. *Cardiovasc Res*. 1994;28:1623–1628.
6. De Carvalho Frimm C, Sun Y, Weber KT. Angiotensin II receptor blockade and myocardial fibrosis of the infarcted rat heart. *J Lab Clin Med*. 1997;129:439–446.
7. Weber KT. Fibrosis, a common pathway to organ failure: angiotensin II and tissue repair. *Semin Nephrol*. 1997;17:467–491.
8. Nishizuka Y. Studies and perspective of protein kinase C. *Science*. 1986;233:305–312.
9. Sadoshima J, Izumo S. Signal transduction pathways of angiotensin II induced c-fos gene expression in cardiac myocytes in vitro: roles of phospholipid-derived second messengers. *Circ Res*. 1993;73:424–438.
10. Crabos M, Roth M, Hahn AW, Erne P. Characterization of angiotensin II receptors in cultured adult rat cardiac fibroblasts: coupling to signaling systems and gene expression. *J Clin Invest*. 1994;93:2372–2378.
11. Imahori Y, Fujii R, Ueda S, et al. Membrane trapping of carbon-11-labeled 1,2-diaclyglycerols as a basic concept for assessing phosphatidylinositol turnover in neurotransmission process. *J Nucl Med*. 1992;33:413–422.
12. Imahori Y, Fujii R, Ueda S, Ohmori Y, Wakita K, Matsumoto K. Phosphoinositide turnover imaging linked to muscarinic cholinergic receptor in the central nervous system by positron emission tomography. *J Nucl Med*. 1993;34:1543–1551.
13. Imahori Y, Ohmori Y, Fujii R, Matsumoto K, Ueda S. Rapid incorporation of carbon-11-labeled diacylglycerol as a probe of signal transduction in glioma. *Cancer Res*. 1995;55:4225–4229.
14. Matsumoto K, Imahori Y, Fujii R, et al. Evaluation of phosphoinositide turnover on ischemic human brain with 1-[1- ^{11}C]-butyryl-2-palmitoyl-rac-glycerol using PET. *J Nucl Med*. 1999;40:1590–1594.
15. Yamane Y, Ishide N, Kagaya Y, et al. Quantitative double-tracer autoradiography with tritium and carbon-14 using imaging plates: application to myocardial metabolic studies in rats. *J Nucl Med*. 1995;36:518–524.
16. Yamane Y, Ishide N, Kagaya Y, et al. Heterogeneous fatty acid uptake early after reperfusion in rat hearts. *Am J Physiol*. 1998;274:H923–H929.
17. Fukuchi M, Hussain SNA, Giaid A. Heterogeneous expression and activity of endothelial and inducible nitric oxide synthesis in end-stage human heart failure: their relation to lesion site and β -adrenergic receptor therapy. *Circulation*. 1998;98:132–139.
18. Ju H, Zhao S, Tappia PS, Panagia V, Dixon IM. Expression of G_{q} and PLC- β in scar and border tissue in heart failure due to myocardial infarction. *Circulation*. 1998;97:892–899.
19. Guaragna RM, Trugo L, Borojevic R. Phospholipid modifications during conversion of hepatic myofibroblasts into lipocytes (Ito-cells). *Biochim Biophys Acta*. 1992;1128:237–243.
20. Prpic V, Weiel JE, Somers SD, et al. Effects of bacterial lipopolysaccharide on the hydrolysis of phosphatidylinositol-4,5-bisphosphate in murine peritoneal macrophages. *J Immunol*. 1987;139:526–533.
21. Namiuchi S, Kagaya Y, Chida M, et al. Regional and temporal profiles of phorbol 12,13-dibutyrate binding after myocardial infarction in rats: effects of captopril treatment. *J Cardiovasc Pharmacol*. 2000;35:353–360.
22. Komuro I, Katoh Y, Kaida T, et al. Mechanical loading stimulates cell hypertrophy and specific gene expression in cultured rat cardiac myocytes: possible role of protein kinase C activation. *J Biol Chem*. 1991;266:1265–1268.
23. Shubeita HE, McDonough PM, Harris AN, et al. Endothelin induction of inositol phospholipid hydrolysis, sarcomere assembly, and cardiac gene expression in ventricular myocytes: a paracrine mechanism for myocardial cell hypertrophy. *J Biol Chem*. 1990;265:20555–20562.
24. LaMorte VJ, Thorburn J, Absher D, et al. G_{q} - and ras-dependent pathways mediate hypertrophy of neonatal rat ventricular myocytes following alpha 1-adrenergic stimulation. *J Biol Chem*. 1994;269:13490–13496.
25. Hee-Cheong M, Severson DL. Metabolism of dioctanoylglycerol by isolated cardiac myocytes. *J Mol Cell Cardiol*. 1989;21:829–837.